Calcium-dependent binding of calmodulin to neuronal gap junction proteins

ARTICLE *in* BIOCHEMICAL AND BIOPHYSICAL RESEARCH COMMUNICATIONS · NOVEMBER 2005

Impact Factor: 2.3 · DOI: 10.1016/j.bbrc.2005.08.007 · Source: PubMed

Published in final edited form as:
Biochem Biophys Res Commun. 2005 October 7; 335(4): 1191–1198.

Calcium-dependent binding of calmodulin to neuronal gap junction proteins

Gary S. Burr[1,†], **Cheryl K. Mitchell**[1], **Yenabi J. Keflemariam**[1], **Ruth Heidelberger**[2,3], and **John O'Brien**[1,3,*]

1 *Department of Ophthalmology and Visual Science, University of Texas Health Science Center at Houston*

2 *Department of Neurobiology and Anatomy, University of Texas Health Science Center at Houston*

3 *The Graduate School of Biomedical Sciences, University of Texas Health Science Center at Houston*

Abstract

We examined the interactions of calmodulin with neuronal gap junction proteins connexin35 (Cx35) from perch, its mouse homologue Cx36, and the related perch Cx34.7 using surface plasmon resonance. Calmodulin bound to the C-terminal domains of all three connexins with rapid kinetics in a concentration- and Ca^{2+}-dependent manner. Dissociation was also very rapid. K_D's for calmodulin binding at a high-affinity site ranged from 11 to 72 nM, and $K_{1/2}$'s for Ca^{2+} were between 3 and 5 μM. No binding to the intracellular loops was observed. Binding competition experiments with synthetic peptides mapped the calmodulin binding site to a 10–30 amino acid segment at the beginning of the C-terminal domain of Cx36. The micromolar $K_{1/2}$'s and rapid on and off rates suggest that this interaction my change dynamically in neurons, and may occur transiently when Ca^{2+} is elevated to a level that would occur in the near vicinity of an activated synapse.

Keywords

Calmodulin; connexins; gap junction; connexin35; connexin36; surface plasmon resonance; calcium; retina

INTRODUCTION

Gap junctions are a critical component of neural circuitry in the retina and central nervous system. Ionic flow through the intercellular channels created by gap junctions mediates electrical coupling between the participating cells, providing for variable sharing of electrical signals. Electrical coupling between neurons is dynamic, and many factors appear to regulate the extent of coupling. The best described of these are the dopamine receptor-mediated changes that regulate coupling, and consequently receptive field size, in horizontal and AII amacrine cells, and some photoreceptors [cf. 1–3]. These operate through protein kinase pathways and depend on phosphorylation at specific sites on the connexin proteins [4].

A number of other factors also regulate gap junctions. Intracellular calcium has long been known to regulate gap junctional coupling. For example, raising intracellular Ca^{2+} to very high levels causes uncoupling of gap junctions in invertebrate neurons, mammalian cell lines, and mammalian neurons [5–7]. In contrast, Ca^{2+} signals are also responsible for the activity-

*Corresponding author: John O'Brien, Department of Ophthalmology and Visual Science, University of Texas Health Science Center at Houston, 6431 Fannin St., MSB 7.024, Houston, Texas 77030, Phone: (713) 500-5983, FAX: (713) 500-0682, e-mail: John.OBrien@uth.tmc.edu.
†Present address: Department of Wildlife and Fisheries Sciences, Texas A&M University, College Station, TX.

dependent *potentiation* of gap junctions in Mauthner cell mixed synapses [8,9], which have recently been shown to contain Cx35 [10]. Thus Ca^{2+} is involved in two distinct physiological mechanisms that can control gap junctional coupling.

One route through which Ca^{2+} may regulate protein function is calmodulin binding. Calmodulin (CaM) is a nearly ubiquitous Ca^{2+}-binding protein that is involved in a myriad of different regulatory pathways, and has been proposed to regulate low-pH induced uncoupling of gap junctions [11,12]. In this study, we have examined the ability of CaM to bind to the cytoplasmic domains of several neuronal connexins that form electrical synapses. These include fish Cx35 and Cx34.7, and mouse Cx36. We find that there is a specific, calcium-dependent interaction between these connexins and CaM.

MATERIALS and METHODS

Protein Expression and Purification

Portions of the cDNAs coding for cytoplasmic domains of perch Cx35 and Cx34.7 and mouse Cx36 were cloned into bacterial expression vectors. For each construct, restriction sites were introduced into the connexin sequences by PCR using Pfu polymerase (Stratagene, La Jolla, CA), and the PCR products subcloned into the expression vector. The carboxyl-terminal domains were cloned into pGexKG (Amersham, Piscataway, NJ), resulting in constructs coding for 33 kDa fusion proteins containing glutathione-S-transferase and amino acids 254–304 of perch Cx35, 253–306 of perch Cx34.7, or 269–321 of mouse Cx36. The intracellular loop domains were cloned into pET42 (Novagen, Madison, WI) and coded for 40 kDa fusion proteins containing a GST tag and amino acids 102–178 of Cx35 or 102–179 of Cx34.7. The fusion proteins were expressed in *E. coli* strain BL21 for pGex clones or BL21(DE3) for pET clones.

GST fusion proteins were purified from bacterial extracts by binding to glutathione sepharose 4B (Amersham). The carboxyl termini were proteolytically degraded in bacteria, so further purification using preparative SDS-PAGE was used to obtain intact C-terminal fusion proteins. The glutathione sepharose-purified proteins were electrophoresed on 12% polyacrylamide gels and negatively stained with a copper staining kit (Bio-Rad, Hercules, CA.). The intact protein bands were excised from the gel and eluted overnight in 50mM Tris, 0.2 M NaCl, 5 mM DTT, 0.1 mM EDTA, 0.1 mg/ml BSA, 0.1% SDS at 4°C. The eluted protein was precipitated with ice-cold acetone, dried, and solubilized in 6 M Guanidine-HCL. The solubilized protein was diluted 50-fold with phosphate buffered saline (PBS) with 65 mM betaine and 0.05% Tween 20, and then dialyzed overnight against PBS plus 0.05% Tween 20, 1 mM dithiothreitol and 10% glycerol to renature the protein.

Calmodulin [13] was a generous gift of Dr. M. Neal Waxham (University of Texas, Houston). The concentration of CaM stock was determined by amino acid analysis at the Baylor College of Medicine protein chemistry core facility.

Binding measurements

Binding interactions were measured by surface plasmon resonance (SPR) using a Biacore 2000 system (Biacore AB, Uppsala, Sweden). Anti-GST antibodies (Amersham) were covalently immobilized on CM5 research grade chips (Biacore) using N-hydroxysuccinamide and 1-ethyl-3(3-dimethylaminopropyl)-carbodiimide (Biacore amine coupling kit). The anti-GST antibodies were immobilized to 6800 to 8100 response units (RU). GST-fusion proteins were subsequently injected over the immobilized antibody to obtain 150–400 RU of fusion protein immobilized. GST was loaded into one of the four flow cells and used as a reference for the remaining flow cells. Prior to performing experiments, we examined the dependence of the

binding responses on mass transport by injecting CaM over the chip at increasing flow rates. Mass transport limitation, evident by increased apparent rates of association with increasing flow rates, was present when connexin C-terminal fusion proteins were loaded onto the chip surface at levels approaching 1000 RU. No mass transport limitation was detected at the loading levels used for our experiments (150–400 RU).

CaM (1 nM to 10 μM) was injected over the sensor surface at a flow rate of 30 μl/minute in binding buffers containing a range of free Ca^{2+} concentrations. The compositions of these buffers are listed in Table 1a. CaM was allowed to interact with the surface of the sensor chip for 1 minute, after which time CaM-free binding buffer was injected over the sensor surface to monitor CaM dissociation. The sensor surface was regenerated using a calcium free flow buffer (140 mM KCl, 10 mM HEPES, 5 mM HEDTA, 5 mM EGTA, 4.62 mM $MgCl_2$, 0.05% Tween 20, pH 7.2; 0.5 mM free Mg^{2+}) between injections. The amount of CaM bound (in RU) was measured as a mean of 10 to 30 sec of data in the steady state phase of the binding curve. These values were used in conjunction with the measurement of connexin domain immobilized and the predicted molecular weights of CaM and the connexin fusion proteins to determine an apparent molar stoichiometry of binding.

For one set of experiments, the pH of the binding buffer was varied from 6.2 to 7.2 at nominal free Ca^{2+} from 1 to 50 μM, with 5 μM CaM and 3 mM Mg^{2+}. The compositions of these binding buffers are listed in Table 1b. In these experiments, the dissociation step was omitted and the flow cells were returned to Ca^{2+}-free flow buffer at pH 7.2 (140 mM KCl, 5 mM HEPES, 5 mM MES, 5 mM HEDTA, 5 mM EGTA, 8.37 mM $MgCl_2$, 0.05% Tween 20, pH 7.2; 3 mM free Mg^{2+}) immediately after binding to reduce low pH-induced loss of fusion protein from the anti-GST surface. To control for such loss, internal standard injections with 50 μM Ca^{2+} at pH 7.2 were interspersed among the sample runs and compared to runs made at the beginning and ending of the experiments. Losses ranged from 2 to 10% over the course of the experiments and were corrected in the final data based on a linear regression of the internal standard binding responses.

For all of the solutions prepared, free Ca^{2+} and Mg^{2+} was calculated using MaxChelator [14] (V. 2.45; available at http://www.stanford.edu/~cpatton/maxc.html) and binding constants file CMC0204.tcm. The free Ca^{2+} in the solutions was independently analyzed with a Ca^{2+} electrode (Microelectrodes, Inc., Bedford, NH) calibrated against standards made from a 0.1 M $CaCl_2$ standard solution (Ricca Chemical Co., Arlington, TX). In some cases, it was necessary to adjust the reported Ca^{2+} concentration to reflect differences between the predicted and measured Ca^{2+} concentrations.

Peptide competition experiments

A series of peptides covering the sequence of the Cx36 C-terminal domain was synthesized at the M.D. Anderson Cancer Center synthetic antigen laboratory. The peptide sequences are shown in Table 3. The ability of these peptides to compete with the connexin C-terminal domains for CaM binding was examined by co-injection of the peptides with 1 μM CaM in binding buffer containing 300 μM free Ca^{2+} (see Table 1a). Peptide concentration was varied from 0.1 μM to 1 mM, except for P1, which was not soluble above 100 μM. The peptides showed some non-specific binding to the chip or the immobilized proteins. This binding was compensated by subtracting the binding signal derived from injections of peptide in the absence of CaM. The specific binding signals were normalized to the binding observed with 1 μM CaM at 300 μM Ca^{2+} in the absence of peptides. IC_{50}'s were determined from exponential fits to the normalized data.

Data Analysis

BIAEvaluation Software (Version 3.1; Biacore) was used to process and analyze raw binding data. Other data analyses were done with Microsoft Excel and Igor Pro (WaveMetrics, Lake Oswego, OR). Steady state calmodulin binding affinity data were analyzed with a general ligand binding model of the form:

$$Y = C + \frac{B\max 1 \cdot [CaM]}{Kd1 + [CaM]} + \frac{B\max 2 \cdot [CaM]}{Kd2 + [CaM]} + \ldots + \frac{B\max n \cdot [CaM]}{Kdn + [CaM]} \quad (1)$$

Data were analyzed assuming one to three binding sites.

RESULTS and DISCUSSION

Calmodulin binds to Cx35 in a Ca^{2+}-dependent manner

Intracellular calcium is an important regulator of coupling through gap junctions made of many types of connexins, and CaM has been proposed to play a role in this regulation [12]. To examine whether CaM might interact with the neuronal gap junctions we examined CaM binding to cytoplasmic domains of perch Cx35 by surface plasmon resonance. The cytoplasmic intracellular loop (IL) and carboxyl terminal (CT) domains of Cx35 were expressed as GST fusion proteins in bacteria, purified, and immobilized on an SPR chip by binding to an anti-GST antibody covalently linked to the chip. Figure 1 shows the binding responses of the IL domain (figure 1A) and the CT domain (figure 1B) to injections of a series of CaM concentrations with 1 mM free Ca^{2+}. The non-specific binding responses to GST and the chip surface have been subtracted out (see Methods). CaM bound to the CT domain in a concentration-dependent manner, with rapid kinetics. Minimal binding to the IL domain was detected. Figure 1C shows that binding to the IL domain appeared to be non-specific while binding to the CT domain showed saturation kinetics typical of specific binding. CaM binding to the CT domain was fit poorly with a single binding site model (dashed line, $X^2 = 0.026$; see Equation 1 for model) but fit well with a two-component ligand binding model (solid line, $X^2 = 0.0015$). The two-component model gave a K_d for CaM of 72 ± 9 nM for the high affinity site and a K_d for CaM of 2.4 ± 0.3 μM for the low affinity site (summarized in Table 2). The presence of a binding site with very low affinity and the relatively low stoichiometry of binding suggest that some of the connexin fusion protein used may be in a non-native conformation that supports calmodulin binding poorly.

Binding of CaM to the Cx35 CT domain was calcium-dependent. In binding experiments in which the Ca^{2+} concentration was varied from 0.1 μM to 1 mM, CaM binding increased with saturation kinetics that could be fit with a Hill equation (figure 2). This fit yielded a $K_{½}$ for Ca^{2+} of 4.9 ± 1.9 μM and a Hill coefficient of 0.69 ± 0.20.

Calmodulin binds to the C-termini of related neuronal connexins

Cx35 is very closely conserved with its mammalian gene homologue Cx36, and is also closely related to a second perch connexin, Cx34.7 [15], that is co-expressed with Cx35 in some retinal neurons [16]. To determine whether these related connexins also bound CaM, we performed binding experiments similar to those described above with intracellular domains of perch Cx34.7 and mouse Cx36. The binding curves in figure 3 (A and C) show that the CT domains of both Cx34.7 and Cx36 also bound CaM with characteristics similar to those of the Cx35 CT domain. Both showed two apparent binding sites (Cx34.7 CT: $X^2 = 0.060$ for one component, $X^2 = 0.0016$ for two components; Cx36 CT: $X^2 = 0.038$ for one component, $X^2 = 0.0066$ for two components). The CaM affinities at the high affinity site were slightly higher for both: 29 ± 2 nM for Cx34.7 CT and 11 ± 3 nM for Cx36 CT. As with Cx35, the IL domain of Cx34.7 did not show specific binding (figure 3A). We did not examine the IL domain of Cx36.

CaM binding to the Cx34.7 and Cx36 CT domains showed calcium-dependence similar to that of Cx35 CT (figure 3B and D). The Hill equation fits for these data revealed Hill coefficients of 1 or less for both connexins, and $K_{½}$ for Ca^{2+} of 3.4 ± 3.1 μM for Cx34.7 and 3.0 ± 0.58 μM for Cx36. The parameters for the binding interactions of CaM with the connexin CT domains are summarized in Table 2. The low Hill coefficient is unusual for calmodulin target binding. The majority of calmodulin binding interactions show positive cooperativity with respect to Ca^{2+}-dependence, reflecting cooperativity in binding Ca^{2+} to calmodulin. Hill coefficients near 1 suggest that binding depends on the association of Ca^{2+} with a single Ca^{2+}-binding site. The slight negative cooperativity seen in some samples may result from the presence of connexin CT domains in a conformation unfavorable to calmodulin binding.

Calmodulin binding is weakly influenced by pH

CaM has been demonstrated to mediate the low pH-induced uncoupling of some gap junction channels [17,18]. Low pH-induced uncoupling is evident in both Cx35 [19] and Cx36 [20], so we examined the effects of pH on CaM binding to the neuronal connexins. Figure 4 shows the effect of reduced pH on binding of 2 μM CaM to Cx34.7, Cx35 and Cx36 CT domains at several Ca^{2+} concentrations. For all three connexins, reduction in pH resulted in a small increase in the molar stoichiometry of binding compared to pH 7.2. This effect was most apparent at pH 6.2, at which pH CaM binding increased 29 to 43% above the pH 7.2 value at 25 μM Ca^{2+}. These results show that CaM binding can be increased by large decreases in intracellular pH. These changes were quite small, however, and suggest that a pH-dependent shift in CaM binding affinity at this site is unlikely to be the basis of the low pH induced uncoupling of gap junctions. This does not exclude the involvement of CaM binding at this site from pH-induced uncoupling, but indicates that such a phenomenon would rely more on an increase in cytoplasmic [Ca^{2+}] than on acidification.

Localization of a calmodulin binding site

The binding curves for all three connexins showed two components, suggesting that there might be more than one calmodulin binding site on the C-termini of the connexins. However, this property could also arise from partially unfolded connexin preparations that contain a single binding site with two different characteristics. To evaluate this question, we mapped the calmodulin binding sites using binding competition experiments. We measured CaM binding in the presence of an overlapping set of 20 amino acid synthetic peptides matching the sequence of the Cx36 C-terminal domain (Table 3). The two peptides closest to the 4^{th} transmembrane domain (P1 and P2) significantly competed with all three connexin CT domains for CaM binding (figure 5A–C), with IC_{50}'s between 2.6 and 9.1 μM (Table 3). P1 had slightly greater ability than P2 to compete for CaM binding to Cx34.7 and Cx35 C-termini. For the Cx36 C-terminal domain, P2 blocked binding with marginally greater efficacy than P1, and P3 also showed a very low ability to compete for CaM binding, with an IC_{50} of 204 μM. P3 did not interfere with CaM binding to the other connexin CT domains, and no effects were seen with P4. These results suggest that the CaM binding site for Cx36 is located within 10–30 aa at the beginning of the C-terminal domain (figure 5D). The minimal core for this binding site includes the region of overlap between P1 and P2, i.e. the sequence WRKIKLAVRG. We found no evidence that there were two separate binding sites; however, we can not rule out that there are two contiguous binding sites.

Calmodulin binding sites are characterized by the presence of basic and bulky hydrophobic residues [21]. The region predicted by the competition experiments to contain the CaM binding site (dashed line in figure 5D) conforms to this description. This site is largely conserved among the three connexins, which could explain why the characteristics of binding were very similar among them. The site is not widely conserved among the connexin gene family as a whole (authors' unpublished analyses).

CaM has been found previously to bind to a number of gap junction proteins [22–25]. In the liver gap junction protein, Cx32, CaM gel overlay experiments indicated that there were at least two CaM binding sites [25]. This was confirmed by peptide binding experiments [26]. Peracchia and coworkers have found CaM to be a key mediator of low pH-induced uncoupling in Cx32 [27], and have further found that this requires an association of CaM with the connexin during or before channel assembly [18,28]. This suggests a stable association of CaM with Cx32.

Torok et al. [26] characterized two CaM binding sites in Cx32 by synthetic peptide binding experiments. This study revealed a striking difference between the two binding sites in that the amino terminal site had a high affinity for CaM (K_d = 27 nM) while the C-terminal site had a substantially lower affinity (K_d = 1.2 μM). Both sites had $K_{½}$'s for Ca^{2+} around 200 nM. The CaM binding site we have identified in Cx35 and its relatives is similar in CaM affinity to the high affinity site on Cx32, but displays more than ten-fold lower $K_{½}$ for Ca^{2+}. This suggests that the CaM binding site on Cx35 will behave quite differently than the Cx32 sites.

The behavior of CaM-target protein interactions depends on a number of factors including the target CaM affinity, the Ca^{2+}-dependence of the interaction, the free [Ca^{2+}], and the concentration of available CaM. The total CaM concentration in cells can exceed 10 μM [29], however much of this may be bound. Recent measurements of CaM in HEK 293 cells with a FRET biosensor indicate that about 8.8 μM CaM, 35%–50% of the total, is available in the resting state [30]. Elevation of cytoplasmic [Ca^{2+}] above 4 μM reduced the CaM available to the biosensor to undetectable levels. In reasonable agreement with these observations, Kim et al. [31] found about 72% of CaM in HEK 293 cells was freely diffusible in a Ca^{2+}-free condition by two photon fluorescence correlation spectroscopy. Elevation of cytoplasmic [Ca^{2+}] shifted the proportion of rapidly diffusible CaM to 50% and reduced the diffusion rate of that component two-fold. Both studies show that the available CaM becomes limited by binding to its targets when [Ca^{2+}] is elevated to high levels. This highlights the concept that the magnitude of CaM-target interactions will be influenced by competition between targets of different abundances and CaM affinities.

The CaM binding site we have found on the neuronal connexin C-termini has moderate affinity for CaM but a high $K_{½}$ for Ca^{2+}. These characteristics suggest that CaM binding to this site will occur when [Ca^{2+}] is elevated to micromolar levels, and may be sensitive to competition with other proteins with higher CaM affinity. Cx35 is present in a number of mixed synapses that contain Ca^{2+}-permeable NMDA receptors [10,32]. Such mixed synapses provide an opportunity for the connexin to experience high Ca^{2+} concentrations both pre- and post-synaptically, and bind to CaM. The physiological consequences of this interaction remain to be elucidated.

Acknowledgements

The authors wish to thank Dr. Neal Waxham for insightful discussions and for the gift of purified calmodulin. The authors also wish to thank Dr. Agnes Puskas and Dr. David Needleman for training and assistance with the Biacore 2000. This research was supported by grants from the National Eye Institute (EY12857, EY012128, and EY10608) and Research to Prevent Blindness. The synthetic antigen facility is supported by NIH core grant CA16672.

References

1. Piccolino M, Neyton J, Gerschenfeld HM. Decrease of gap junction permeability induced by dopamine and cyclic adenosine 3′:5′-monophosphate in horizontal cells of turtle retina. J Neurosci 1984;4:2477–2488. [PubMed: 6092564]
2. Hampson EC, Vaney DI, Weiler R. Dopaminergic modulation of gap junction permeability between amacrine cells in mammalian retina. Journal of Neuroscience 1992;12:4911–4922. [PubMed: 1281499]

3. Krizaj D, Gabriel R, Owen WG, Witkovsky P. Dopamine D2 receptor-mediated modulation of rod-cone coupling in the Xenopus retina. J Comp Neurol 1998;398:529–538. [PubMed: 9717707]
4. Ouyang X, Winbow VM, Patel LS, Burr GS, Mitchell CK, O'Brien J. Protein kinase A mediates regulation of gap junctions containing connexin35 through a complex pathway. Brain Res Mol Brain Res 2005;135:1–11. [PubMed: 15857663]
5. Baux G, Simonneau M, Tauc L, Segundo JP. Uncoupling of electrotonic synapses by calcium. Proc Natl Acad Sci U S A 1978;75:4577–4581. [PubMed: 279937]
6. Flagg-Newton J, Loewenstein WR. Experimental depression of junctional membrane permeability in mammalian cell culture. A study with tracer molecules in the 300 to 800 Dalton range. J Membr Biol 1979;50:65–100. [PubMed: 41101]
7. Rao G, Barnes CA, McNaughton BL. Occlusion of hippocampal electrical junctions by intracellular calcium injection. Brain Res 1987;408:267–270. [PubMed: 3109688]
8. Yang XD, Korn H, Faber DS. Long-term potentiation of electrotonic coupling at mixed synapses. Nature 1990;348:542–545. [PubMed: 2174130]
9. Pereda AE, Faber DS. Activity-dependent short-term enhancement of intercellular coupling. J Neurosci 1996;16:983–992. [PubMed: 8558267]
10. Pereda A, O'Brien J, Nagy JI, Bukauskas F, Davidson KG, Kamasawa N, Yasumura T, Rash JE. Connexin35 mediates electrical transmission at mixed synapses on Mauthner cells. J Neurosci 2003;23:7489–7503. [PubMed: 12930787]
11. Peracchia C. Calmodulin-like proteins and communicating junctions. Electrical uncoupling of crayfish septate axons is inhibited by the calmodulin inhibitor W7 and is not affected by cyclic nucleotides. Pflugers Arch 1987;408:379–385. [PubMed: 3035483]
12. Peracchia C. Chemical gating of gap junction channels; roles of calcium, pH and calmodulin. Biochim Biophys Acta 2004;1662:61–80. [PubMed: 15033579]
13. Gaertner TR, Putkey JA, Waxham MN. RC3/Neurogranin and Ca2+/calmodulin-dependent protein kinase II produce opposing effects on the affinity of calmodulin for calcium. J Biol Chem 2004;279:39374–39382. [PubMed: 15262982]
14. Patton C, Thompson S, Epel D. Some precautions in using chelators to buffer metals in biological solutions. Cell Calcium 2004;35:427–431. [PubMed: 15003852]
15. O'Brien J, Bruzzone R, White TW, Al-Ubaidi MR, Ripps H. Cloning and expression of two related connexins from the perch retina define a distinct subgroup of the connexin family. J Neurosci 1998;18:7625–7637. [PubMed: 9742134]
16. O'Brien J, Nguyen HB, Mills SL. Cone photoreceptors in bass retina use two connexins to mediate electrical coupling. J Neurosci 2004;24:5632–5642. [PubMed: 15201336]
17. Peracchia C, Wang X, Li L, Peracchia LL. Inhibition of calmodulin expression prevents low-pH-induced gap junction uncoupling in Xenopus oocytes. Pflugers Arch 1996;431:379–387. [PubMed: 8584431]
18. Peracchia C, Sotkis A, Wang XG, Peracchia LL, Persechini A. Calmodulin directly gates gap junction channels. J Biol Chem 2000;275:26220–26224. [PubMed: 10852921]
19. White TW, Deans MR, O'Brien J, Al-Ubaidi MR, Goodenough DA, Ripps H, Bruzzone R. Functional characteristics of skate connexin35, a member of the γ subfamily of connexins expressed in the vertebrate retina. Eur J Neurosci 1999;11:1883–1890. [PubMed: 10336656]
20. Teubner B, Degen J, Sohl G, Guldenagel M, Bukauskas FF, Trexler EB, Verselis VK, De Zeeuw CI, Lee CG, Kozak CA, Petrasch-Parwez E, Dermietzel R, Willecke K. Functional expression of the murine connexin 36 gene coding for a neuron-specific gap junctional protein. J Membr Biol 2000;176:249–262. [PubMed: 10931976]
21. Rhoads AR, Friedberg F. Sequence motifs for calmodulin recognition. Faseb J 1997;11:331–340. [PubMed: 9141499]
22. Hertzberg EL, Gilula NB. Liver gap junctions and lens fiber junctions: comparative analysis and calmodulin interaction. Cold Spring Harb Symp Quant Biol 1982;46(Pt 2):639–645. [PubMed: 6955103]
23. Welsh MJ, Aster JC, Ireland M, Alcala J, Maisel H. Calmodulin binds to chick lens gap junction protein in a calcium- independent manner. Science 1982;216:642–644. [PubMed: 6280283]

24. Van Eldik LJ, Hertzberg EL, Berdan RC, Gilula NB. Interaction of calmodulin and other calcium-modulated proteins with mammalian and arthropod junctional membrane proteins. Biochem Biophys Res Commun 1985;126:825–832. [PubMed: 2983692]
25. Zimmer DB, Green CR, Evans WH, Gilula NB. Topological analysis of the major protein in isolated intact rat liver gap junctions and gap junction-derived single membrane structures. J Biol Chem 1987;262:7751–7763. [PubMed: 3034905]
26. Torok K, Stauffer K, Evans WH. Connexin 32 of gap junctions contains two cytoplasmic calmodulin-binding domains. Biochem J 1997;326:479–483. [PubMed: 9291121]
27. Peracchia C, Wang XC. Connexin domains relevant to the chemical gating of gap junction channels. Braz J Med Biol Res 1997;30:577–590. [PubMed: 9283624]
28. Sotkis A, Wang XG, Yasumura T, Peracchia LL, Persechini A, Rash JE, Peracchia C. Calmodulin colocalizes with connexins and plays a direct role in gap junction channel gating. Cell Adhes Commun 2001;8:277–281.
29. Chin D, Means AR. Calmodulin: a prototypical calcium sensor. Trends Cell Biol 2000;10:322–328. [PubMed: 10884684]
30. Black DJ, Tran QK, Persechini A. Monitoring the total available calmodulin concentration in intact cells over the physiological range in free Ca2+ Cell Calcium 2004;35:415–425. [PubMed: 15003851]
31. Kim SA, Heinze KG, Waxham MN, Schwille P. Intracellular calmodulin availability accessed with two-photon cross-correlation. Proc Natl Acad Sci U S A 2004;101:105–110. [PubMed: 14695888]
32. Pereda A, O'Brien J, Nagy JI, Smith M, Bukauskas F, Davidson KG, Kamasawa N, Yasumura T, Rash JE. Short-range functional interaction between connexin35 and neighboring chemical synapses. Cell Commun Adhes 2003;10:419–423. [PubMed: 14681051]

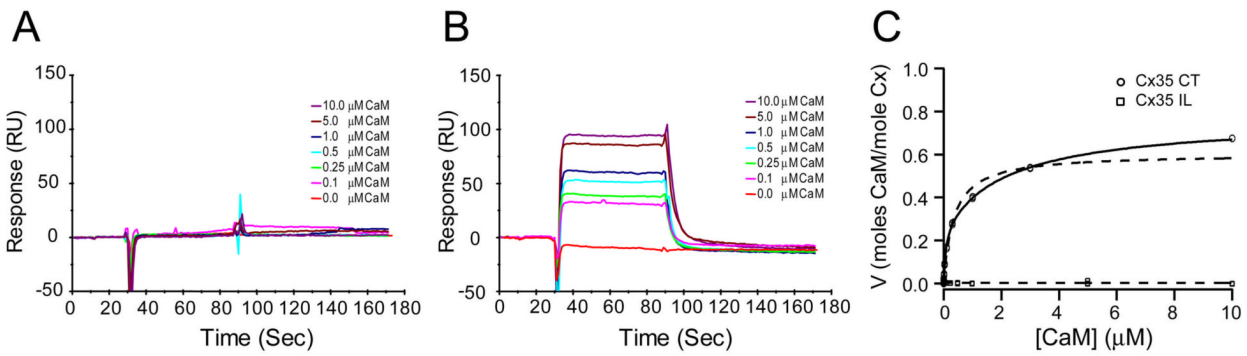

Figure 1. Calmodulin binding to Cx35 cytoplasmic domains

A. A family of SPR traces showing steady state binding responses of the Cx35 intracellular loop domain GST fusion protein (1070 RU immobilized) to calmodulin ranging from 0 to 10 μM in buffer containing 1 mM free Ca^{2+}. Responses to GST alone have been subtracted.

B. A similar family of SPR traces showing binding responses of the Cx35 C-terminal domain GST fusion protein (344 RU immobilized) to 0 to 10 μM calmodulin in buffer containing 1 mM free Ca^{2+}. Responses to GST alone have been subtracted as in A.

C. Steady state CaM binding data for 10 [CaM] from 1 nM to 10 μM for Cx35 CT, and for 6 [CaM] from 100 nM to 10 μM for Cx35 IL. The fits of a single-component ligand binding model to the Cx35 CT and IL data are shown by the dashed lines; the fit for a two-component model to the CT data is shown by the solid line. Parameters for the two-component fit are shown in Table 2.

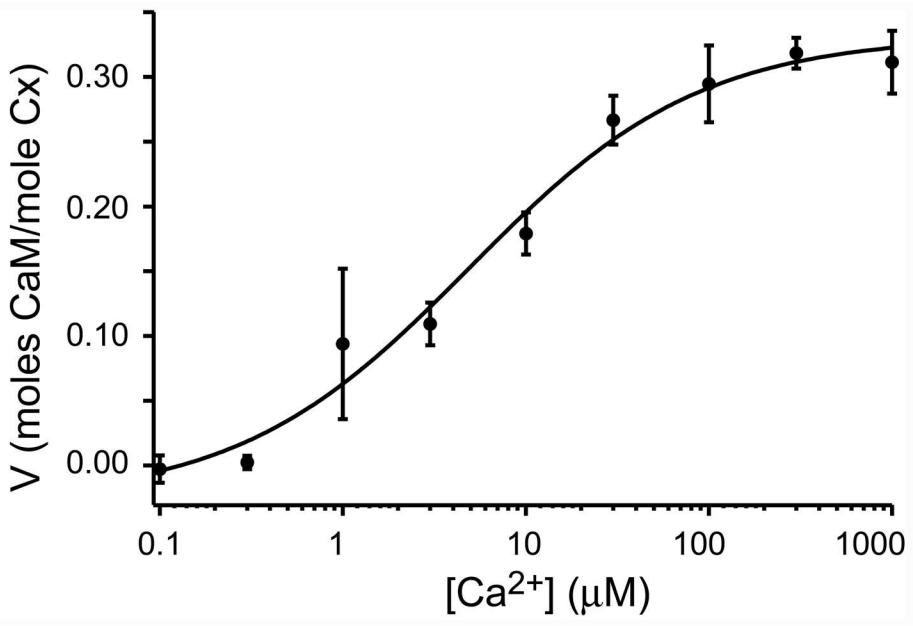

Figure 2. Calcium dependence of CaM binding to the Cx35 CT domain

Specific binding responses of the Cx35 CT domain to injections of 2 μM CaM in solutions containing 0.1 μM to 1 mM free Ca^{2+}. The curve fit to the data represents a Hill equation with a $K_{½}$ for Ca^{2+} of 4.9 ± 1.9 μM, saturation value of 0.33 ± 0.02 moles CaM/mole Cx, and a Hill coefficient of 0.69 ± 0.20. Data are means of 6 measurements ± 1 SD.

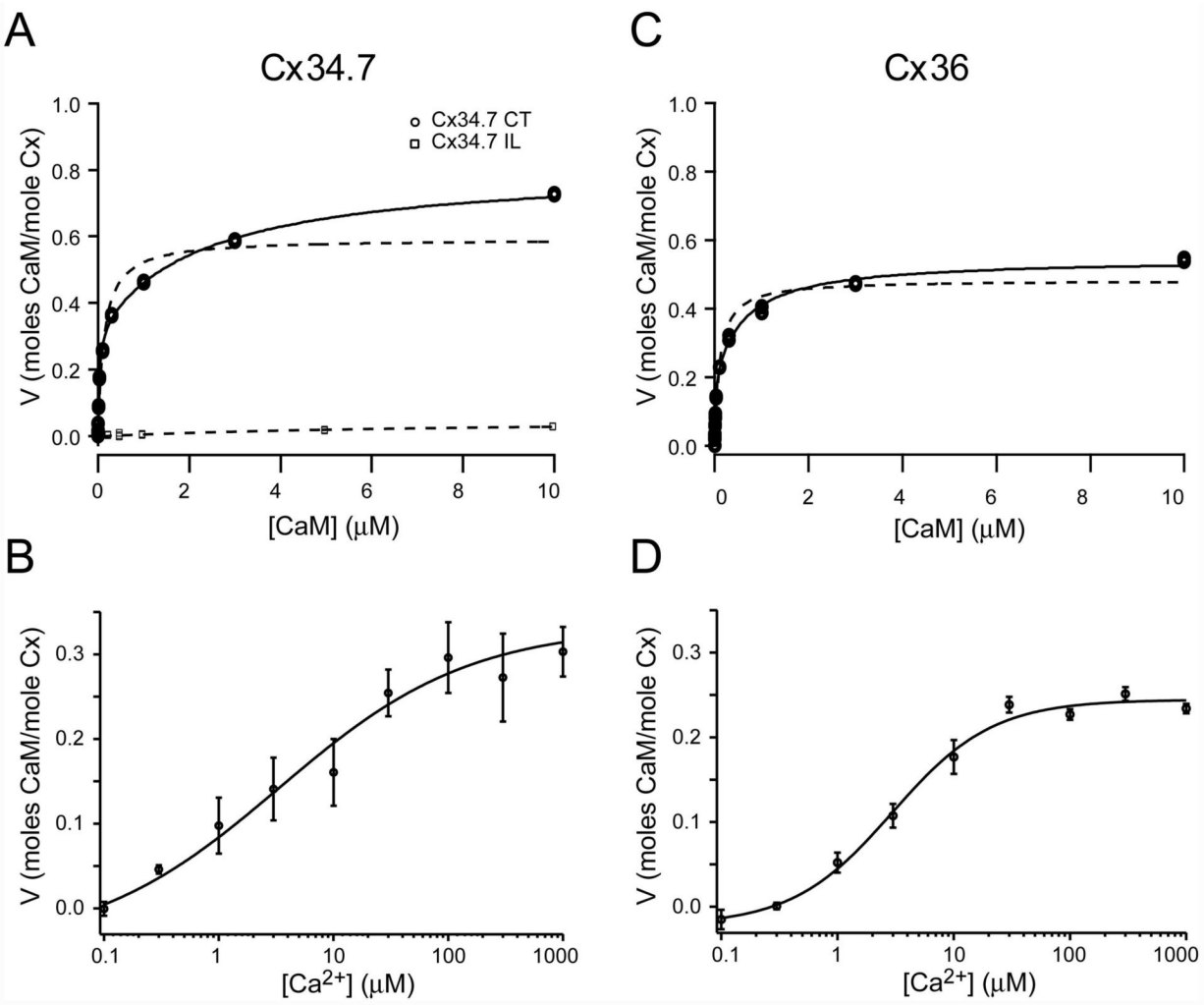

Figure 3. Calmodulin binding to Cx34.7 and Cx36 cytoplasmic domains

A. Steady state binding curves for the Cx34.7 CT and IL domains. Binding conditions, CaM concentrations, and data analysis are as in figure 1. Parameters for the two-component binding model fit to the Cx34.7 CT domain are shown in Table 2.

B. Calcium-dependence of CaM binding to Cx34.7 CT domain. Conditions are as described in figure 2. The curve fit is a Hill equation with $K_{½}$ for Ca^{2+} of 3.4 ± 3.1 μM, saturation value of 0.33 ± 0.05 moles CaM/mole Cx, and a Hill coefficient of 0.52 ± 0.28.

C. Steady state CaM binding curve for the Cx36 CT domain. Binding conditions, CaM concentrations, and data analysis are as in figure 1. Parameters for the two-component binding model fit to the Cx34.7 CT domain are shown in Table 2.

D. Calcium-dependence of CaM binding to Cx36 CT domain. Conditions are as described in figure 2. The curve fit represents a Hill equation with $K_{½}$ for Ca^{2+} of 3.0 ± 0.6 μM, saturation value of 0.24 ± 0.01 moles CaM/mole Cx, and a Hill coefficient of 1.01 ± 0.18.

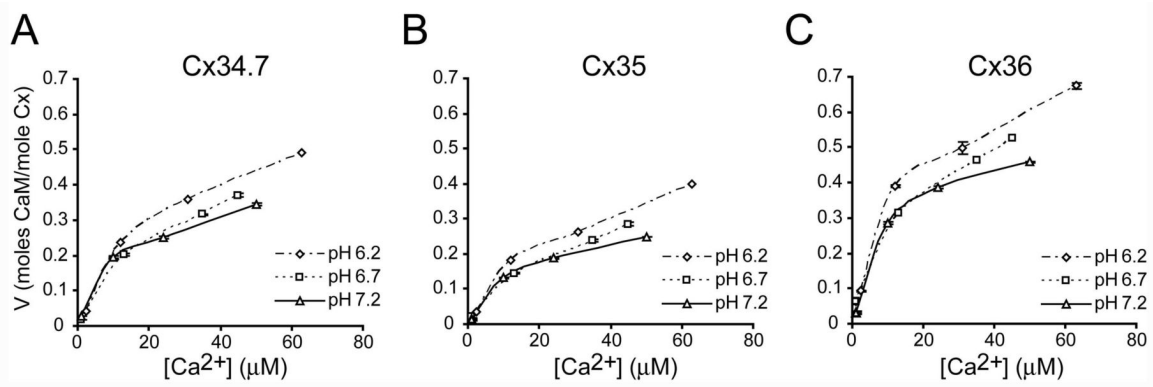

Figure 4. pH dependence of CaM binding to connexin CT domains

Calcium-dependence of steady-state binding of 1.6 μM CaM to the CT domains of Cx34.7 (A), Cx35 (B), and Cx36 (C) at three pH's. Data shown are means of three measurements ± 1 SD.

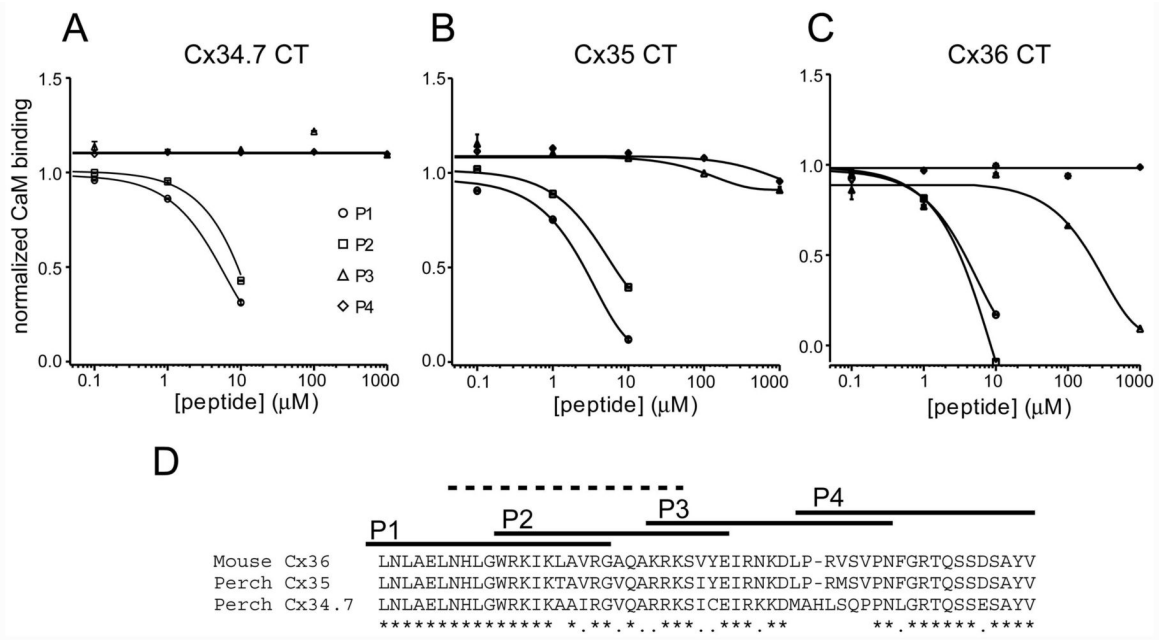

Figure 5. Identification of a calmodulin binding site through binding competition

Steady state binding responses of Cx34.7 CT domain (A), Cx35 CT domain (B) and Cx36 CT domain (C) to injections of 1 μM CaM in 300 μM Ca^{2+} buffer in the presence of synthetic peptides matching portions of the Cx36 CT domain sequence. Peptide sequences are shown in Table 3 and are represented in the figure by the abbreviations P1–P4. The key in panel A applies to A–C. Binding responses are normalized to the response to 1 μM CaM in 300 μM Ca^{2+} buffer in the absence of peptide. IC_{50}'s calculated from the exponential curves fit to the data are shown in Table 3.

D. Amino acid alignment of the full C-terminal domains of perch Cx35, mouse Cx36 and perch Cx34.7, beginning with the last three amino acids predicted to be within transmembrane domain 4. Symbols below the alignment indicate amino acids that are identically conserved (*) and those that have similar character (.). The positions of the peptides P1–P4 used for binding competition experiments are shown by bars above the alignment. A calmodulin binding site predicted by the binding competition experiment is indicated by the dashed line.

Table 1

A. Solutions for Ca^{2+}-dependence of binding										
Nominal Free Ca^{2+}	**0.1 μM**	**0.3 μM**	**1 μM**	**3 μM**	**10 μM**	**30 μM**	**100 μM**	**300 μM**	**1 mM**	**Flow buffer**
KCl	140	140	140	140	140	140	140	140	140	140
MOPS (pH 7.2)	10	10	10	10	10	10	10	10	10	10
HEDTA	5	5	5	5	5	5	5	5	5	5
EGTA	5	5	5	5	--	--	--	--	--	5
NTA	--	--	--	--	5	5	5	5	5	--
$CaCl_2$	1.69	3.04	4.27	4.98	1.00	2.34	4.62	6.99	9.54	0.0
$MgCl_2$	4.58	4.54	4.46	4.30	4.70	3.81	2.50	1.52	0.906	4.62
Tween 20	0.05%	0.05%	0.05%	0.05%	0.05%	0.05%	0.05%	0.05%	0.05%	0.05%
Free Mg^{2+}	0.50	0.50	0.50	0.50	0.50	0.50	0.50	0.50	0.50	0.50

B. Solutions for pH-dependence of binding												
Nominal Free Ca^{2+}	**1 μM**			**10 μM**			**25 μM**			**50 μM**		
pH	7.2	6.7	6.2	7.2	6.7	6.2	7.2	6.7	6.2	7.2	6.7	6.2
KCl	140	140	140	140	140	140	140	140	140	140	140	140
HEPES	5	5	5	5	5	5	5	5	5	5	5	5
MES	5	5	5	5	5	5	5	5	5	5	5	5
HEDTA	5	5	5	5	5	5	5	5	5	5	5	5
EGTA	5	5	--	5	5	5	5	5	5	--	--	--
NTA	--	--	--	--	--	--	--	--	--	5	5	5
EDTA	--	--	5	--	--	--	--	--	--	--	--	--
$CaCl_2$	4.13	1.73	0.14	5.10	4.38	1.90	5.38	5.10	3.23	1.26	1.04	0.77
$MgCl_2$	7.84	7.50	11.2	7.57	7.60	6.40	7.43	7.07	6.23	9.57	8.13	6.59
Tween 20	0.05 %	0.05 %	0.05 %	0.05 %	0.05 %	0.05 %	0.05 %	0.05 %	0.05 %	0.05 %	0.05 %	0.05 %
Free Mg^{2+}	3.00	3.00	3.00	2.99	3.01	3.00	3.00	2.99	2.99	3.00	3.00	3.00
Measured free Ca^{2+} (μM)	1	1	2.4	10	13	12	24	35	31	50	45	63

Table 2

Parameters of steady-state calmodulin binding

	Cx34.7 CT	Cx35 CT	Cx36 CT
[1] K_D (CaM) low affinity site	29 ± 2 nM	72 ± 9 nM	11 ± 3 nM
[1] Bmax (CaM) low affinity site	0.32 ± 0.01	0.27 ± 0.02	0.19 ± 0.02
[1] K_D (CaM) high affinity site	2.35 ± 0.26 μM	2.39 ± 0.33 μM	0.60 ± 0.13 μM
[1] Bmax (CaM) low affinity site	0.49 ± 0.01	0.50 ± 0.02	0.36 ± 0.02
[2] $K_{½}$ for Ca^{2+}	3.4 ± 3.1 μM	4.9 ± 1.9 μM	3.0 ± 0.6 μM
Hill coefficient[3]	0.52 ± 0.28	0.69 ± 0.20	1.01 ± 0.18

[1] K_D and Bmax determined at 1 mM free Ca^{2+}

[2] Determined from Hill fit

[3] For Ca^{2+}-dependence of calmodulin binding

Table 3

Competition of peptides for CaM binding[1].

Peptide sequence	IC_{50} Cx34.7CT	IC_{50} Cx35CT	IC_{50} Cx36CT
P1: GILAELNHLGWRKIKLAVRG[2]	5.3 μM	2.6 μM	3.7 μM
P2: WRKIKLAVRGAQAKRKSVYE	9.1 μM	6.5 μM	3.2 μM
P3: KRKSVYEIRNKDLPRVSVPN	n.d.	n.d.	204 μM
P4: LPRVSVPNFGRTQSSDSAYV	n.d.	n.d.	n.d.

[1] 1 μM CaM at 300 μM free Ca^{2+}.

[2] The first two aa of P1 are coded for by the GST fusion vector.